ELSEVIER

Polymer 40 (1999) 5207–5211

polymer

Polymer Communication

Grafted polymer tail/loop mixtures differing in chain length

Daniel C. Driscoll[a], Harpreet S. Gulati[b], Richard J. Spontak[a,b,*], Carol K. Hall[b]

[a]*Department of Materials Science & Engineering, North Carolina State University, Raleigh, NC 27695-7907, USA*
[b]*Department of Chemical Engineering, North Carolina State University, Raleigh, NC 27695-7905, USA*

Received 7 October 1998; received in revised form 17 November 1998; accepted 17 November 1998

Abstract

Studies examining the structure of monolayers formed by polymer chains grafted to a surface typically focus on chains attached at one end (*tails*). Bond fluctuation simulations are performed here to probe monolayers composed of equimolar mixtures of tails and double-grafted *loops* in which the looped chain length (N_{loop}) is varied at constant surface density and tail length (N_{tail}). Loops force the tails to adopt an extended trajectory normal to the surface, resulting in monolayer stratification. As N_{loop} increases, the height of the tail sublayer increases to a maximum, and then decreases to converge with the loop sublayer as $N_{loop} \rightarrow 2N_{tail}$. These results are compared to predictions from a self-consistent field theory for bidisperse mixtures of grafted tails.

Keywords: Grafted polymer chains; Brushes; Polymer thin films

1. Introduction

Numerous theoretical, simulation and experimental efforts have demonstrated that the properties of an impenetrable surface can be readily modified through the use of polymer chains that are chemically attached, or grafted, to the surface. Polymer chains are grafted to an inorganic surface through the use of specific (e.g. acid–base or ionic) interactions at selected "sticky" sites along the chain backbone [1,2], and are utilized to tailor the properties governing adhesion [3], colloidal stabilization [4,5] and hydrophilicity [6]. Moreover, chains grafted to a surface can likewise be employed in the development of "smart" nanoscale devices that operate on the swelling response of polymers to different solvents [7]. These evolving applications require that the height and structure of thin polymer monolayers be precisely controlled at nanometer length scales. Such control can be achieved through the use of monofunctionalized chains so that each chain attaches at one end and behaves as a *tail* [8]. Extensive theoretica1 [8–14] and simulation [13,15–18] efforts have sought to elucidate the molecular factors responsible for the dense packing of mono- and polydisperse tails at a surface and have, as an additional benefit, provided insight into the microdomain structure of microphase-ordered block copolymer mixtures [19–23].

If a chain is functionalized at both ends, then it attaches to the surface at two sites and forms a more highly constrained polymer *loop*. Relatively few studies have examined the equilibrium [24] and dynamic [25] properties of loops, since loops are often treated as tails of half chain length. This approximation accurately yields the conformational properties of loops at low surface density (σ) and chain length (N) [24], as well as of looped blocks in ordered block copolymers [26,27]. It fails, however, to account for differences in chain diffusion, relaxation time and extension between loops and tails when density saturation effects arise at high σ and N [25]. Since loops and tails can exhibit dissimilar properties, bond-fluctuation (BF) simulations have been performed [28] to discern the roles of mixture composition (x_{loop}), σ and N on the equilibrium features of tail/loop mixtures in which the tail and loop chain lengths are equal (i.e. $N = N_{tail} = N_{loop}$). Such a system likewise describes an ensemble of dual-end-functionalized chains in which only some of the chains re-enter the monolayer to form loops [29]. Predictions from the self-consistent field (SCF) formalism of Lai and Zhulina [13] for tail mixtures differing in N by a factor of 2 agree with the BF results at low σ and N, but deviate modestly from the simulations as σ and N increase beyond the point of chain impingement. In this work, we present BF simulations for tail/loop mixtures in which N_{loop} is varied at constant x_{loop}, σ and N_{tail}, and compare the results with SCF predictions for bidisperse tail mixtures.

* Corresponding author.

0032-3861/99/$ - see front matter
PII: S0032-3861(98)00804-0

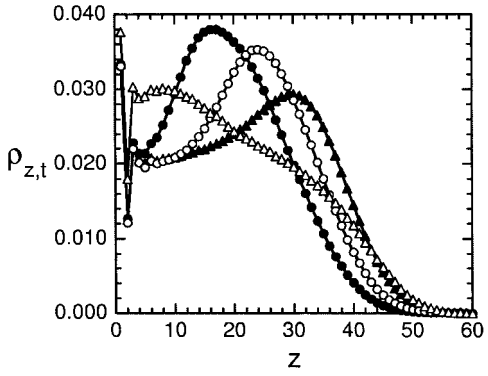

Fig. 1. Segmental density distributions for grafted polymer tails ($\rho_{z,t}$) in four equimolar tail/loop mixtures with different chain length ratios (η): 0.5 (●), 1.0 (○), 1.5 (▲) and 2.0 (△). In each case, $N_{tail} = 40$ and $\sigma = 0.086$. The solid lines serve as guides for the eye.

2. Simulation procedure

The BF model [24,30,31] used here to simulate equimolar polymer tail/loop mixtures grafted to an impenetrable surface in the presence of a good solvent employs a three-dimensional periodic cell in which the surface measures 50×50 lattice parameters. The cell height is maintained larger than the length of the fully extended tails when oriented normal to the surface (along the $+z$ direction). This on-lattice Monte Carlo algorithm allows bond length and direction to fluctuate insofar as the bond lengths lie within 2 to $\sqrt{10}$ lattice parameters and the bond vectors remain in the set {(2,0,0), (2,1,0), (2,1,1), (2,2,1), (3,0,0), and (3,1,0)}. Due to enhanced flexibility, the BF model closely emulates off-lattice simulations [25,31]. As described elsewhere [24,28], the polymer chains are initially arranged (at random) in an extended conformation normal to the surface at $z = 0$: tails as straight chains of N_{tail} beads, and loops as hairpins of N_{loop} beads ($N_{loop}/2$ beads comprise the sides of the hairpin normal to the surface and connect at the top by a bond of length 2). The grafted sites diffuse laterally along the surface during system relaxation and simulation, which proceeds when a random bead on a random chain is selected and moved by one step in a random direction. A move is valid if: (i) the new bond vector lies in the set listed above, and (ii) the new site is not occupied by another bead. Equilibrium is achieved according to the protocol established [24] for polymer loops: three independent simulation runs are averaged to ensure chain and layer characteristics remain constant within 1% variation.

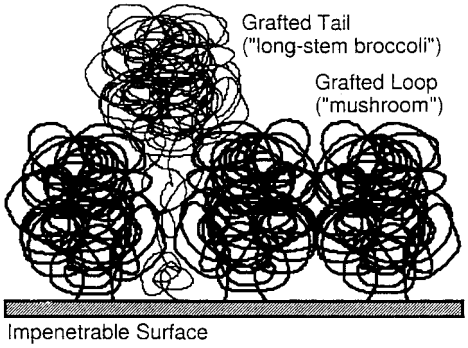

Fig. 2. Schematic illustration of a mixture of polymer loops and tails grafted to an impenetrable surface. For $\eta < 2.0$ within the scaling regime, the chains are laterally compressed and form loop- and tail-rich sublayers, in which the loops adopt a *mushroom* conformation near the surface and the tails are squeezed to form long-stem *broccoli*, as depicted here.

3. Results and discussion

Segmental density distributions for tails ($\rho_{z,t}$), normalized so that $\int_0^\infty \rho_{z,t} dz = 1$, are presented in Fig. 1 for four equimolar (50/50) tail/loop mixtures with chain length ratios ($\eta = N_{loop}/N_{tail}$) of 0.5, 1.0, 1.5 and 2.0. Throughout this study, N_{tail} and σ are maintained constant at 40 and 0.086, respectively, where σ is defined in terms of the number of chains, *not* graft sites, attached to the surface at $z = 0$. Since the critical impingement density of a comparable system (composed solely of looped chains [24]) is exceeded, adjacent chains (tails or loops) in the mixtures examined here are expected to interact with one another by excluding available volume. Within this so-called "scaling" regime, the monolayer densifies as the constituent chains, each desiring to adopt a *mushroom*-shaped conformation, become laterally compressed. Such compression in unary chain ensembles yields segmental density distributions that follow a parabolic trajectory [5,11,25]. None of the $\rho_{z,t}$ distributions shown in Fig. 1, however, exhibits a classical parabolic trajectory due to stratification of the monolayer, in which the loops form an inner sublayer in close proximity to the surface at $z = 0$ and the tails form an outer boundary layer. Monolayer stratification is predicted for bidisperse tail mixtures [12–14], and has been observed [28] in BF simulations of tail/loop mixtures for which $\eta = 1$.

Over the range $0.5 \leq \eta \leq 1.5$, each of the tail segmental distributions in Fig. 1 exhibits a maximum density along z. The position of the peak is closely associated with the location at which the loop sublayer terminates, and increases with increasing η due to enlargement of the inner sublayer. In contrast, the peak magnitude decreases with increasing η due to conservation of the number of tail segments. At distances beyond the peak density in each mixture, $\rho_{z,t}$ decays according to a classical parabolic trajectory, implying that the tail segments within the boundary sublayer adopt a less perturbed conformation along z than those stretched segments residing in the inner sublayer. Therefore, loop-induced volume exclusion is responsible for the tails appearing as long-stemmed *broccoli*, adopting a highly extended conformation within, and a more relaxed conformation above, the loop sublayer, as illustrated in Fig. 2. The same is not true, however, for the mixture in which the loop sublayer extends out to the boundary sublayer ($\eta = 2.0$). In this case, $\rho_{z,t}$ exhibits a shallow maximum near the surface at $z = 0$ and a shoulder near $z \approx 35$. A maximum in $\rho_{z,t}$ near

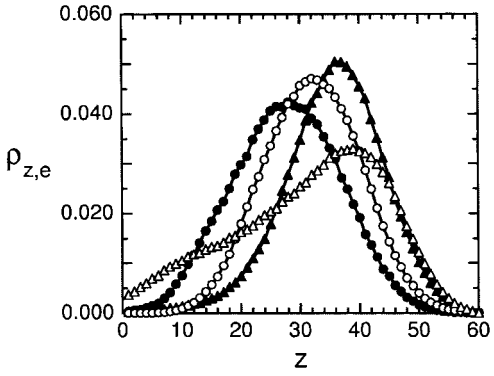

Fig. 3. End-bead density distributions of grafted tails in the mixtures described in Fig. 1 (using the same symbols). The solid lines are guides for the eye.

the surface indicates that a substantial fraction of tail segments (larger than any of the other three cases in Fig. 1) lies in close proximity to the surface, as would occur in a system composed entirely of tails. The presence of double-stranded loops in the $\eta = 2.0$ mixture still causes the tails to extend slightly near the top of the monolayer, thereby resulting in the shoulder evident in $\rho_{z,t}$ in the vicinity of $z \approx 35$.

Similar results are gleaned from the normalized end-bead distribution functions ($\rho_{z,e}$) corresponding to the mixtures displayed in Fig. 1. These distributions are provided in Fig. 3 and reveal that the ends of the tails are pushed further outward (along z) as η is increased from 0.5 to 1.5. Moreover, an increase in η is accompanied by an increase in the magnitude of the peak density, a shift in the onset of the distribution to higher z, and a reduction in the breadth of the distribution. An interesting feature is that these distributions are all relatively symmetric, regardless of η. When $\eta = 2.0$, however, $\rho_{z,e}$ appears highly asymmetric with a nonzero onset at the surface ($z = 0$) and a maximum beyond the peak density of the $\eta = 1.5$ mixture. A nonzero onset at $z = 0$ indicates that some tail ends in the mixture return to the surface. This result constitutes an important consideration in sequential dual-end-functionalized chain grafting [29], and

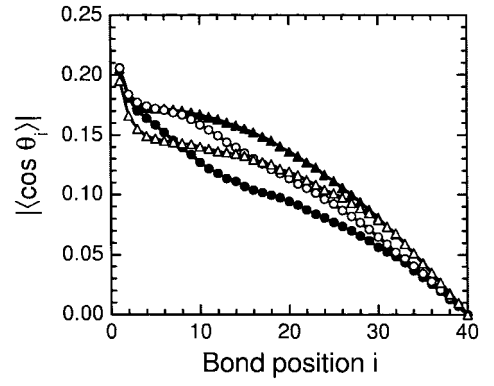

Fig. 4. Local stretching of the grafted tails, as discerned from the absolute mean projection of the ith bond vector normal to the surface ($|\langle\cos\theta_i\rangle|$), for the mixtures described in Fig. 1 (using the same symbols). The solid lines serve as guides for the eye.

is consistent with an increase in tail segments near the surface as $\eta \rightarrow 2.0$ (see Fig. 1).

Local bond stretching provides additional insight into the conformations of grafted chains and is conveniently expressed in terms of the cosine of the angle between the ith bond vector and the direction normal to the surface [13,25], designated $\cos\theta_i$. In general, $\cos\theta_i$ increases as chains extend away from the surface and bonds align normal to the surface, thereby providing a sensitive measure of local chain stretching within the sublayers of a given grafted polymer mixture. The absolute mean projection of the ith bond vector normal to the interface, denoted $|\langle\cos\theta_i\rangle|$, is presented in Fig. 4 as a function of bond position i for the tails in the four mixtures examined previously. As η is increased from 0.5 to 1.5, $|\langle\cos\theta_i\rangle|$ increases for all $i > 6$, in which case the tails become more highly extended normal to the surface as the inner sublayer is enlarged, in agreement with the data presented in Figs. 1 and 3. When η is increased from 1.5 to 2.0, the local bond stretching decreases abruptly for i between 1 and 30 (within the inner sublayer, according to Fig. 1), but remains invariant for $i > 30$ (within the boundary sublayer). According to these data, the tails in the $\eta = 2.0$ mixture are generally less stretched away from the surface than those in the $\eta = 1.5$ mixture. Comparison of the $|\langle\cos\theta_i\rangle|$ data for the $\eta = 0.5$ and $\eta = 2.0$ mixtures reveals that the near-surface tail segments in the $\eta = 2.0$ mixture are more highly compressed normal to the surface (due to the presence of large, accommodating loops) than are those in the $\eta = 0.5$ mixture (with smaller, more compact loops). The remaining tail segments in the $\eta = 2.0$ mixture are, however, more highly stretched away from the surface.

We next explore the effect of loop chain length on the inner (loop) and boundary (tail) sublayer heights in equimolar tail/loop mixtures with varying η. For this purpose, we introduce the first moment of the segmental density profile, defined as $\langle z\rangle = \int_0^\infty z\rho_z(z)dz$, as a measure of layer height. Values of $\langle z\rangle$ for the loop and tail sublayers are shown in Fig. 5. As η is increased, both sublayers initially increase in height due to enlargement of the inner sublayer and extension of the tails. For values of η between 1.0 and 2.0, $\langle z\rangle_{loop}$ increases monotonically, whereas $\langle z\rangle_{tail}$ increases, reaches a maximum and then decreases to where it coincides with $\langle z\rangle_{loop}$ at $\eta = 2.0$. The maximum in $\langle z\rangle_{tail}\eta$ corresponds to the point where the conformational entropy arising from volume exclusion (which is responsible for monolayer stratification) is balanced by the entropy associated with mixing loops and tails of comparable extension. Also shown in Fig. 5 are predictions from the self-consistent field (SCF) formalism of Lai and Zhulina [13] for a bidisperse mixture of tails of lengths N_L and N_S, where the subscripts refer to long (L) and short (S). Recent efforts have shown [28] that simulated segmental distributions and layer heights of tail/loop mixtures with $\eta = 1.0$ are accurately predicted by this theory.

To account for looped chains in the mixture, several SCF

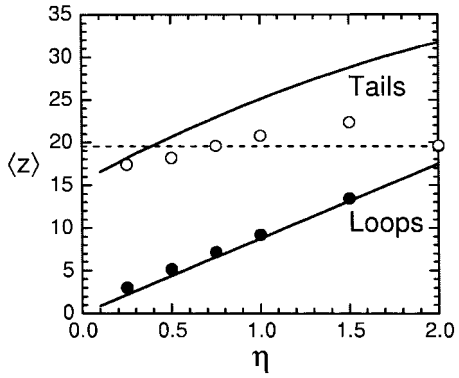

Fig. 5. Average layer heights $\langle z\rangle_{loop}$ (●) and $\langle z\rangle_{tail}$ (○) provided as a function of chain length ratio (η) for equimolar tail/loop mixtures with $N_{tail} = 40$ and $\sigma = 0.086$. The solid lines are predictions from the SCF theory proposed by Lai and Zhulina [13] for a bidisperse mixture of grafted tails, and the dashed (horizontal) line denotes the value of $\langle z\rangle$ evaluated at $\eta = 2.0$, where $\langle z\rangle_{tail} \approx \langle z\rangle_{loop}$.

parameters must be adjusted. For example, $\alpha \equiv (N_L/N_S) - 1$ provides a measure of chain length disparity, wherein $N_L = N_{tail}$ and $N_S = N_{loop}/2$. Since $N_{loop} = \eta N_{tail}$ ($N_{tail} = 40$), N_S can be written as 20η, yielding $\alpha = (2/\eta) - 1$. Each loop of length N_{loop} behaves as two tails of length N_S, in which case the equivalent SCF surface density (σ_{eq}) is given by $\sigma(1 + x_{loop})$, which is equal to 0.129. Likewise, the fraction of long chains (x_L) in the mixture is $1 - 2x_{loop}/(1 + x_{loop}) = 0.333$. Expressions for the inner ($\langle z\rangle_S$) and boundary ($\langle z\rangle_L$) sublayer heights in a bidisperse tail mixture have been derived by Lai and Zhulina: [13]

$$\langle z\rangle_S = \frac{3h_o}{4\pi\varepsilon_3}\left[\left(x_L^{1/3} - 2x_L\right)\varepsilon_2^{1/2} + \tan^{-1}\left(\varepsilon_2^{1/2}/x_L^{1/3}\right)\right] \quad (1)$$

$$\langle z\rangle_L = \frac{3h_o}{16x_L(1+\alpha)}\left[2 + 2\alpha(x_L^{1/3} + x_L + \alpha x_L^{4/3}) + \alpha\varepsilon_2^2\ln(\varepsilon_1/\gamma_1)\right] - \frac{\varepsilon_3\langle z\rangle_S}{x_L(1+\alpha)} \quad (2)$$

where $h_o = (8p\upsilon\sigma_{eq}/\pi^2)^{1/3}N_S$, $\epsilon_j = 1 - x_L^{j/3}$ and $\gamma_j = 1 + x_L^{j/3}$. Molecular properties referred to in these relationships include the chain stiffness parameter (p) and the second virial coefficient (υ). The value of the product $p\upsilon$ used [13] in these SCF calculations is 31.2, in which case $h_o = 29.663\eta$. Values of $\langle z\rangle_S$ and $\langle z\rangle_L$ calculated from Eqs. 1 and 2 are included for comparison with the simulation results in Fig. 5. Predicted $\langle z\rangle_S$ are seen to agree remarkably well with the BF data for $\langle z\rangle_{loop}$ over the entire range of η examined. The same is not true, however, for the predicted $\langle z\rangle_L$, especially as η is increased from 1.0 to 2.0. In fact, neither the maximum in $\langle z\rangle_{tail}$ observed in the simulations nor the convergence of $\langle z\rangle_{tail}$ and $\langle z\rangle_{loop}$ at $\eta = 2.0$ is predicted by this SCF theory, due, most likely, to the mean-field (infinite chain length) approximations inherent in its framework.

4. Conclusions

Bond-fluctuation simulations have been performed here to probe the equilibrium conformational properties of equimolar mixtures of polymer tails and loops grafted to an impenetrable surface. The segmental density distribution results obtained here reveal that the presence of loops in tail/loop mixtures serves to stratify the polymer monolayer at values of η below 2.0. In addition, the tails adopt an increasingly extended conformation as η is increased to just below 2.0 (due to enlargement of the inner sublayer) and then relax considerably to coexist with the loops in a single layer at $\eta = 2.0$. A maximum in the height of the tail sublayer, corresponding to the point where the conformational entropy responsible for monolayer stratification is balanced by the entropy of mixing chains of comparable extension, is found to exist by the simulations performed here, but is not predicted by the SCF formalism of Lai and Zhulina [13] for an analogous bidisperse mixture of grafted tails.

Acknowledgements

This work was supported by the U.S. Department of Energy and the Petroleum Research Fund of the American Chemical Society. We thank Mr A. G. Erlat for technical assistance.

References

[1] Pispas S, Hadjichristidis N. Macromolecules 1994;27:1891.
[2] Stouffer JM, McCarthy TJ. Macromolecules 1988;21:1204.
[3] Garbassi F, Morra M, Occhiello E. Polymer surfaces: from physics to technology, chap. 10. New York: Wiley, 1994.
[4] Fleer GJ, Scheutjens JMHM. Coll Surf 1990;51:281.
[5] Zhulina EB, Borisov OV, Priamitsyn VA. J Coll Interface Sci 1990;137:495.
[6] Ito Y. In: Imanishi Y, editor. Synthesis of biocomposite materials, chap. 1. Boca Raton, FL: CRC Press, 1992.
[7] Israels R, Gersappe D, Fasolka M, Roberts VA, Balazs AC. Macromolecules 1994;27:6679.
[8] Milner ST. Science 1991;251:905.
[9] Alexander S. J Phys II (Fr) 1977;38:983.
[10] de Gennes PG. Macromolecules 1980;13:1070.
[11] Milner ST, Witten TA, Cates ME. Macromolecules 1988;21:2610.
[12] Milner ST, Witten TA, Cates ME. Macromolecules 1989;22:853.
[13] Lai PY, Zhulina EB. Macromolecules 1992;25:5201.
[14] Dan N, Tirrell M. Macromolecules 1993;26:6467.
[15] Murat M, Grest GS. Phys Rev Lett 1989;63:1074.
[16] Murat M, Grest GS. Macromolecules 1991;24:704.
[17] Marko JF, Chakrabarti A. Phys Rev Lett 1993;48:2739.
[18] Binder K, Milchev A, Baschnagel J. Annu Rev Mater Sci 1996;26:107.
[19] Vilesov AD, Floudas G, Pakula T, Melenevskaya E Yu, Birshtein TM, Lyatskaya Yu V. Macromol Chem Phys 1994;195:2317.
[20] Spontak RJ. Macromolecules 1994;27:6363.
[21] Matsen MW. J Chem Phys 1995;103:3268.
[22] Spontak RJ, Fung JC, Braunfeld MB, Sedat JW, Agard DA, Kane L, Smith SD, Satkowski MM, Ashraf A, Hajduk DA, Gruner SM. Macromolecules 1996;29:4494.

[23] Kane L, Satkowski MM, Smith SD, Spontak RJ. Macromolecules 1996;29:8862.
[24] Jones RL, Spontak RJ. J Chem Phys 1995;103:5137.
[25] Gulati HS, Hall CK, Jones RL, Spontak RJ. J Chem Phys 1996;105:7712.
[26] Marko JF. Macromolecules 1993;26:1442.
[27] Matsen MW. J Chem Phys 1995;102:3884.
[28] Driscoll DC, Gulati HS, Spontak RJ, Hall CK. Polymer 1998;39:6339.
[29] Skvortsov AM, Pavlushkov IV, Gorbunov AA, Zhulina EB. J Chem Phys 1996;105:2219.
[30] Carmesin I, Kremer K. Macromolecules 1988;21:2189.
[31] Deutsch HP, Binder K. J Chem Phys 1991;94:2294.